

CALCULATION OF TWO- AND THREE-DIMENSIONAL TRANSONIC CASCADE
FLOW FIELD USING THE NAVIER-STOKES EQUATIONS*

B. C. Weinberg, R.-J. Yang, S.J. Shamroth and H. McDonald
Scientific Research Associates, Inc.

INTRODUCTION

Major objectives of the HOST program have been to improve hot section performance and life. Of specific interest here is the turbine, and in order to achieve the HOST objectives, accurate determinations of turbine blade pressure distributions and associated heat transfer rates are required. Over the years, substantial efforts have been expended in developing reliable and efficient computational procedures for predicting the flow field and accompanying heat transfer characteristics within turbine passages.

At the present time there are three possible approaches to the prediction of turbine flow fields, i.e. (i) inviscid analyses, (ii) inviscid analyses with boundary layer corrections, and (iii) full Navier-Stokes flow field analyses. The first approach is only useful in computing blade loading, and limited by the need to assume airfoil circulation to obtain a unique flow field, and the inability to account for viscous effects. The second approach can be used to obtain heat transfer rates and viscous losses by using either a viscous-inviscid interaction model or a non-interactive technique. The non-interactive technique is viable if viscous displacement effects are small. If the viscous displacement effects are large, then an interaction model should be used. However, this approach is subject to the principal difficulties that the boundary layer approximations may not be valid, and the division between viscous and inviscid regions could be unrealistic. This may be a particular problem in three-dimensional transonic flow where the local pressure distribution and shock location become very sensitive to small changes in the effective passage area. The third approach using the full Navier-Stokes equations solves the flow field using a single set of governing equations requiring no interaction model or approximations in separated regions.

APPROACH

The present work applies a Navier-Stokes analysis [1] employing the time-dependent Linearized Block Implicit scheme (LBI) of Briley and McDonald [2] to two-dimensional and three-dimensional transonic turbulent cascade flows. In general, the geometrical configuration of the turbine blade impacts both the grid construction procedure and the implementation of the numerical algorithm. Since modern turbine blades of interest, e.g. the Allison C3X turbine cascade shown in Fig. 1, are characterized by very blunt leading edges, rounded trailing edges and high stacking angles, a robust grid construction procedure is required that can accommodate the severe body shape while resolving regions of large flow gradients. A constructive O-type grid generation technique, suitable for cascades with rounded trailing edges, has been developed

*Work performed as part of the HOST program (Contract No. NAS3-23695) under sub-contract to the Allison Gas Turbine Division of General Motors.

and used to construct the C3X turbine cascade coordinate grid shown in Fig. 1. The C3X was selected in view of the extensive heat transfer measurement program being undertaken on this airfoil by Allison as part of the HOST program.

Another aspect of the numerical algorithm that is addressed is the setting of boundary conditions; on the body, upstream and downstream boundaries and the periodic surfaces. In particular in the transonic regime, where the pressure on the blade is sensitive to the upstream and downstream conditions proper boundary condition specification is crucial in obtaining accurate predictions. Two-dimensional calculations were performed employing the Navier-Stokes procedure for the C3X turbine cascade, and the predicted pressure coefficients and heat transfer rates were compared with the experimental data generated under the HOST program by Hylton, et al [3]. In addition, the corresponding three-dimensional rectilinear C3X turbine cascade was considered in which blade-endwall effects are present. Three-dimensional Navier-Stokes calculations also were performed. Some results of both the two- and three-dimensional calculations are briefly discussed below.

Figure 1 shows the O-type grid generated by the constructive technique for the C3X blade. The features of the techniques are: (a) the actual physical shape of blade is maintained, (b) regions of large flow gradients are resolved, (c) upstream and downstream boundaries are placed far from the blade surface so that boundary conditions can be more easily implemented, and (d) the coordinate intersection angles are controlled so that metric data associated with the coordinate system are smooth. The coordinate system for two-dimensional calculations consists of 30 points in the pseudo-radial direction and 120 points in the pseudo-azimuthal direction. The upstream boundary is placed at 2.25 axial chords upstream of the leading edge and the downstream boundary is placed at 2.65 axial chords downstream of the trailing edge. High radial resolution is obtained near the surface of the blade, with the first coordinate line located at a distance of 1.0×10^{-6} axial chords from the surface which is within the turbulent boundary layer viscous sublayer. In addition, high pseudo-azimuthal resolution is obtained at both leading and trailing edges.

RESULTS

In Fig. 2 the computed pressure distribution for a sample case (ratio of upstream total to downstream static pressure $P_0/P_{\text{exit}} = 1.66$, exit Mach number $M_{\text{exit}} = 0.9$, exit Reynolds number $Re_{\text{exit}} = 2.43 \times 10^6$, ratio of averaged blade surface temperature to inlet gas total temperature $T_w/T_g = 0.75$, and averaged inlet turbulence intensity $T_u = 6.5\%$, is shown and compared with the Allison experimental data corresponding to case 144 in Ref. 3 and inviscid calculations [4]. There is excellent agreement between the present calculations and the experimental data. Mixing length and $k-\epsilon$ two-equation turbulence models were employed, and (as expected) the results of calculations indicate very little difference in the prediction of the pressure coefficient. Due to the small viscous displacement effect, the inviscid calculations show close agreement with the present computed results. Also shown in this figure are the data from cases 148 and 158 which were run under nominally identical conditions (cf. Ref. 3) to indicate the relationship between the predictions and the experimental scatter.

In Fig. 3 the distribution of the computed heat transfer coefficient is shown for case 144 with both film-cooling and non-film-cooling options. For the non-film-cooling option, with the local surface temperature distribution given in [3], a mixing length turbulence model in conjunction with a transition model was employed in which laminar flow was assumed in the region $X/C_x < 0.2$ followed by a transitional zone and thereafter by fully turbulent flow. The predictions obtained with the model compare very well with the experimental data taken with no film cooling present.

Following this initial calculation, the film cooling option in the code was activated with air injected at 30° to the suction side over $0.8 < x/c_x < 0.9$ at a velocity of 7% of freestream. The local surface temperature was kept fixed at the same value as the non-film-cooling option. Although no data is available for comparison the calculation does demonstrate the effect of film-cooling. From the onset of injection to the trailing edge the heat transfer rate drops to nearly zero. This behavior is a consequence of the buffer region of constant temperature cool gas which protects the blade surface from the hotter fluid in the cascade passage. The comparison of the pressure distribution for both film cooling and non-film-cooling options is shown in Fig. 4. The effect of blowing on the pressure distribution is clear, i.e. the adverse pressure gradient that is generated, the resulting upstream influence, and the subsequent favorable pressure gradient that follows it.

For the three-dimensional rectilinear C3X turbine cascade, the configuration consisted of a C3X cascade situated in the azimuthal-radial plane (see Fig. 1), and bounded in the transverse direction by an endwall and a symmetry plane. For the three-dimensional calculation a grid was constructed consisting of $100 \times 25 \times 15$ grid points in the pseudo-azimuthal, pseudo-radial and transverse directions, respectively. For this demonstration case laminar conditions were assumed. The height of the blade above the endwall (to the symmetry plane, midspan) was set to be one axial chord, while the inlet boundary layer thickness was 20% of that value. The computed pressure distribution at different heights above the endwall are shown in Fig. 5. The pressure side is minimally affected by the endwall, remaining at or near the two-dimensional value run on the same spanwise cross-sectional grid, while the suction side, which shows as much as 15% change over the two-dimensional value near the 30% axial chord location, approaches the two-dimensional value at 26% span above the endwall. The differences from the two-dimensional value are due to the effects of secondary flow generated by horseshoe and passage vortices. The results are consistent with the expected physics (Refs. 5, 6). In Fig. 6, the velocity vector plots are presented for the forward portion of the C3X cascade at two different planes above the endwall. Very near the endwall (within 2.95% spanwise plane) a saddle point exists as indicated in the picture. This saddle point moves toward the leading edge and disappears beyond 2.95% spanwise plane. A stagnation point forms on the nose of the blade surface beyond 2.95% spanwise plane. Further results and a detailed discussion will be presented in the final report, now in preparation.

PLANS

The demonstration three-dimensional calculations completes the technical effort under the subcontract. Future efforts have been proposed and these include continued code development (incorporating the effect of rotation), further validation, improvements in numerical methodology, application to specialized design problems and developing user-oriented input output routines.

REFERENCES

1. Shamroth, S.J., McDonald, H. and Briley, W.R.: Prediction of Cascade Flow Fields Using the Averaged Navier-Stokes Equations. ASME Journal of Engineering for Gas Turbines and Power, Vol. 196, pp. 383-390, 1984.
2. Briley, W.R. and McDonald, H.: Solution of the Multidimensional Compressible Navier-Stokes Equations by a Generalized Implicit Method. Journal of Computational Physics, Vol. 24, pp. 372-397, 1977.
3. Hylton, L.D., Mihelc, M.S., Turner, E.R., Nealy, D.A. and York, R.E.: Analytical and Experimental Evaluation of the Heat Transfer Distribution Over the Surface of Turbine Vanes. NASA-CR-168015, May 1983.
4. Delaney, R.A.: Time Marching Analysis of Steady Transonic Flow in Turbomachinery Cascades Using the Hopscotch Method. ASME Journal of Engineering for Power, Vol. 105, pp. 272-279, 1983.
5. Langston, L.S., Nice, M.L. and Hooper, R.M.: Three-Dimensional Flow Within a Turbine Cascade Passage. ASME Journal of Engineering for Power, Vol. 99, pp. 21-28, 1977.
6. Sieverding, C.H. and Van den Bosche, P.: The Use of Colored Smoke to Visualize Secondary Flows in a Turbine-Blade Cascade. Journal of Fluid Mechanics, Vol. 134, pp. 85-89, 1983.

ORIGINAL PAGE IS
OF POOR QUALITY

C3X TURBINE BLADE "O"-GRID MESH

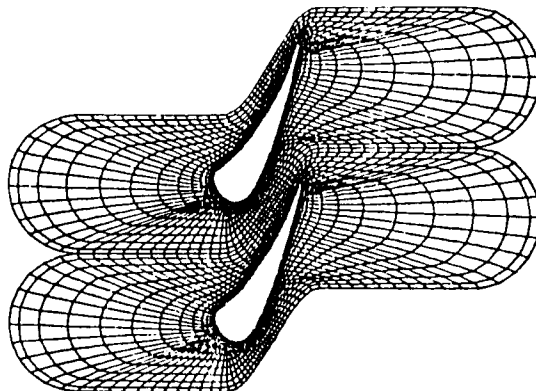


FIGURE 1

PRESSURE COEFFICIENT DISTRIBUTION

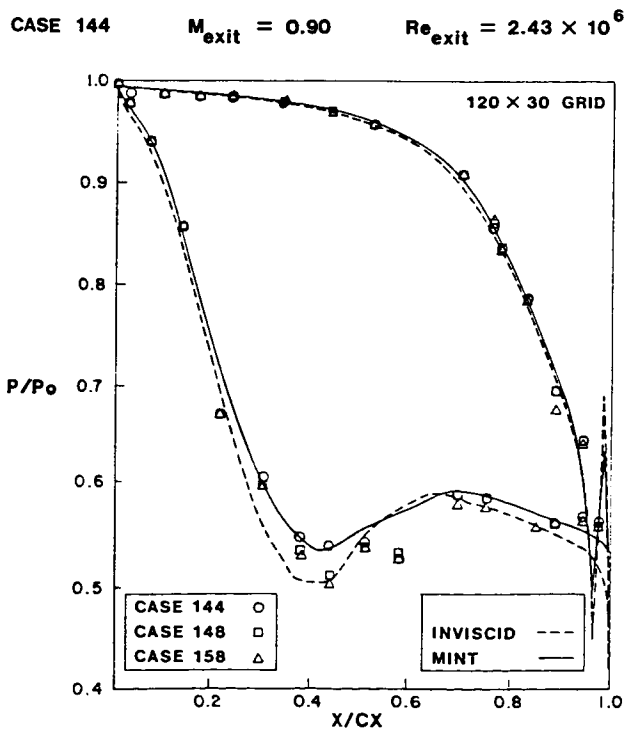


FIGURE 2

HEAT TRANSFER COEFFICIENT

CASE 144

$M_{exit} = 0.90$

$Re_{exit} = 2.43 \times 10^6$

$T_w/T_g = 0.75$

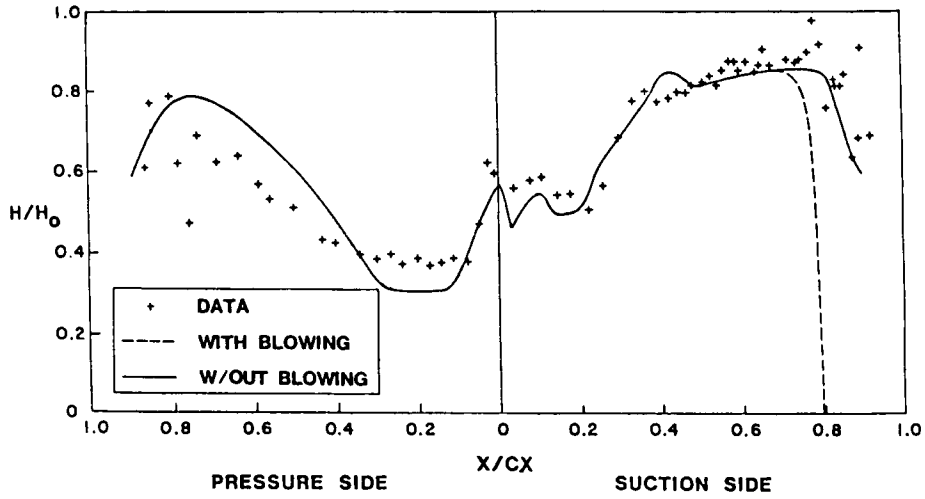


FIGURE 3

PRESSURE COEFFICIENT DISTRIBUTION

CASE 144

$M_{exit} = 0.90$

$Re_{exit} = 2.43 \times 10^6$

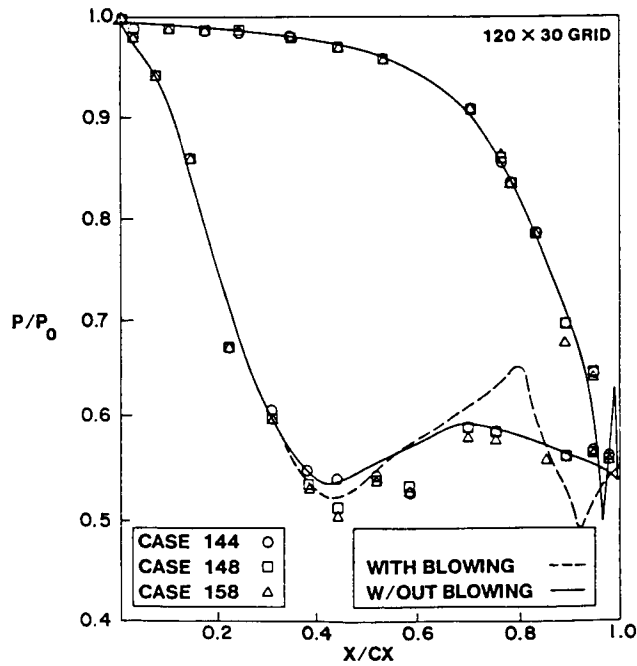


FIGURE 4

**C3X 3-D RECTILINEAR CASCADE
PRESSURE COEFFICIENT DISTRIBUTION**

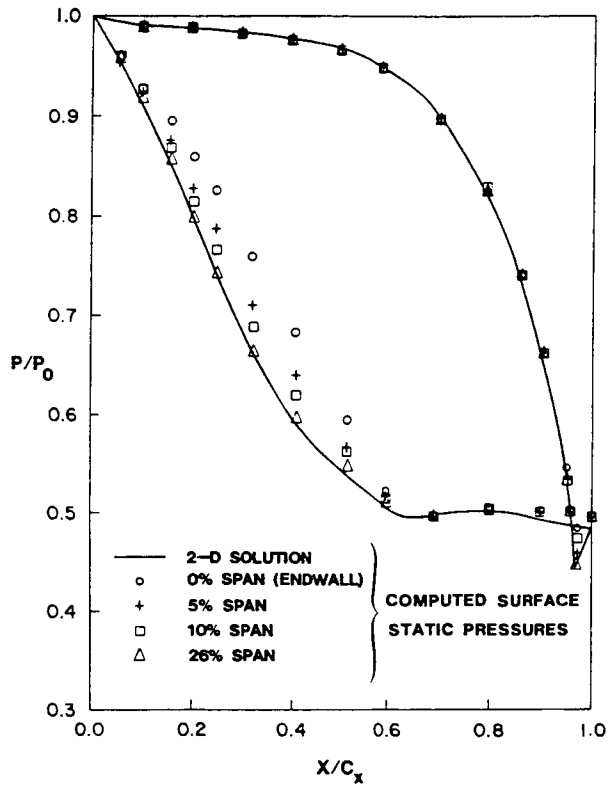
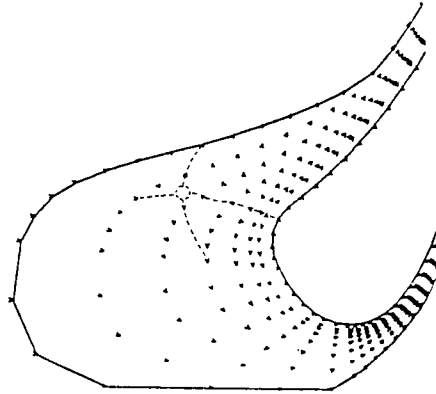
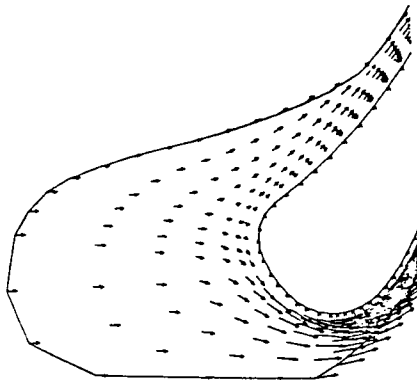


FIGURE 5



(a) VECTOR PLOT ON 0.135% SPANWISE PLANE



(b) VECTOR PLOT ON MIDSPAN PLANE

FIGURE 6